A PARYLENE BELLOWS ELECTROCHEMICAL ACTUATOR FOR INTRAOCULAR DRUG DELIVERY

P.-Y. Li[1], R. Sheybani[2], J.T.W. Kuo[2], and E. Meng[1,2]*
[1]Department of Electrical Engineering, University of Southern California, Los Angeles, California, USA
[2]Department of Biomedical Engineering, University of Southern California, Los Angeles, California, USA

ABSTRACT

The first electrochemical actuator with a Parylene bellows for intraocular drug delivery is presented in which the bellows separates the electrolysis actuation chamber from the drug reservoir. The Parylene bellows was fabricated using a novel polyethylene glycol (PEG)-molding process and mechanically characterized. Optimization of the gas generation efficiency of the actuators was performed. We achieved an efficiency approaching 80% and over 1.5 mm deflection with our actuator. Wireless operation was also demonstrated.

KEYWORDS

Drug Delivery Device, Electrolysis Pump, Bellows, Intraocular Implant

INTRODUCTION

Water electrolysis using coplanar microelectrodes offers a promising pumping actuation mechanism for many bioMEMS applications [1, 2]. Electrolysis actuators possess a simple structure for ease of fabrication, low power consumption, low heat generation, and large driving force.

Previously, we reported the first MEMS electrochemically-driven drug delivery device capable of targeted delivery to intraocular tissues [3]. The system consisted of a drug reservoir integrated with an electrolysis pump and Parylene cannula. The application of current initiated electrolysis of the drug solution which produced the necessary driving pressure to pump drug through the cannula and into the eye (Figure 1).

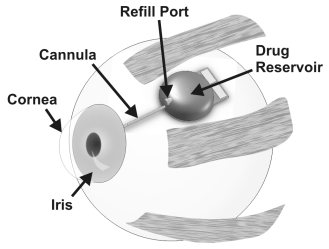

Figure 1: Conceptual depiction of an intraocular drug delivery device.

While the drug delivery concept was successfully demonstrated, several challenges related to the micropump design were identified during preliminary *in vitro* and *in vivo* experiments. First, drug was oxidized by the electrolysis reaction. Power was supplied through wires from an external source and thus, severely limited the ability to conduct chronic *in vivo* experiments. Electrode dimensions were arbitrarily selected; therefore, power consumption of the pump was not optimized. These issues are addressed in our new actuator described here.

DESIGN, THEORY, AND MODELING

The key features of our new, optimized pump actuator include (1) separation of the electrochemical reaction and drug with (2) a robust, high deflection Parylene bellows to prevent unwanted pH changes or drug degradation, (3) an efficiency-optimized electrochemical actuator electrode design, and (4) lower power consumption for long term wireless operation.

The main body of the drug delivery system is implanted within the layers of the eye wall and the attached cannula is inserted through an incision and directed to the intraocular space. The actuator is contained within the main body and is in contact with the contents of the drug reservoir. Electrolysis-induced gas generation (phase change of water into hydrogen and oxygen gas) results in deflection of the bellows and thus pumping of the drug into the eye. Drug is carried directly to the targeted intraocular tissues through the cannula.

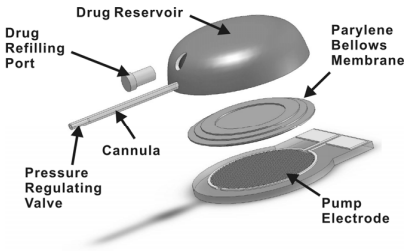

Figure 2: An exploded view of the major system components.

The pump actuator consists of interdigitated Pt electrodes and Parylene bellows that are fabricated separately. The chamber formed by the bellows and electrode base is filled with deionized (DI) water and then joined together (Figure 2). Electrolysis pumping is selected over other actuation methods for its low power consumption (~μW-mW) which makes it suitable for wireless operation and integration with other chronically implantable devices (Figure 3). In addition, current control of electrolysis provides a facile means of adjusting the flow rate.

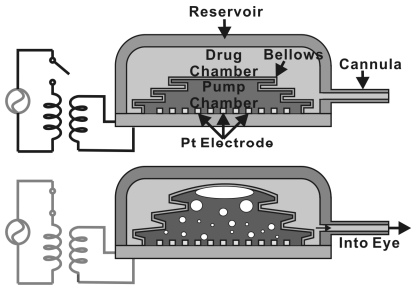

Figure 3: Illustration of the operation principle of the intraocular drug delivery system under wireless power.

Design parameters that determine the pumping efficiency of the interdigitated electrodes and the mechanical performance of the Parylene bellows are discussed. The efficiency (η) of an electrolysis actuator is defined as

$$\eta = \frac{V_{\text{experimental}}}{V_{\text{theoretical}}} \tag{1}$$

where $V_{\text{experimental}}$ is the total volume of the generated hydrogen and oxygen gases and $V_{\text{theoretical}}$ is the theoretical volume of the generated gas bubbles [2]. Factors affecting efficiency of electrochemical systems include electrode design (geometry), external parameters (temperature), electrolysis solution (concentration), and electrical parameters (current) [4]. The interdigitated electrode geometry (specifically electrode width and spacing) was investigated as the other variables were previously reported the literature [5].

Corrugated membranes and bellows were evaluated; however, bellows were selected as the actuator diaphragm for its superior deflection with lower material stress based on nonlinear FEM analyses using quarter models (Figure 4). Bellows achieved greater deflection compared to corrugated membranes (1.5 mm vs. 0.8 mm for 10 µm thick membranes) under 0.5 psi (3.44 kPa) applied pressure. The maximum stress in the bellows was 61.8 MPa (<68.9 MPa tensile strength of Parylene). The linear bellows approximation [6] is

$$\delta = 2n\left[\frac{3(1-\nu^2)}{16}\left(1-\frac{b^4}{a^4}-4\frac{b^2}{a^2}\ln\frac{a}{b}\right)\right]\frac{Pa^4}{Eh^3} \tag{2}$$

where δ is the bellows deflection, n is the number of the convolutions, ν is the Poisson's ratio, a is the inner radius of the bellows, b is the outer radius of the bellows, P is the uniform applied pressure, E is the Young's modulus of Parylene, and h is the thickness of the Parylene bellows.

FABRICATION AND PACKAGING

Pump Electrodes

Interdigitated electrodes were fabricated on glass substrates by liftoff (Figure 5). A dual-layer photoresist process was used to create an undercut for liftoff. Then Ti/Pt film (300 Å/2000 Å) was e-beam evaporated. The pump electrodes were defined by liftoff.

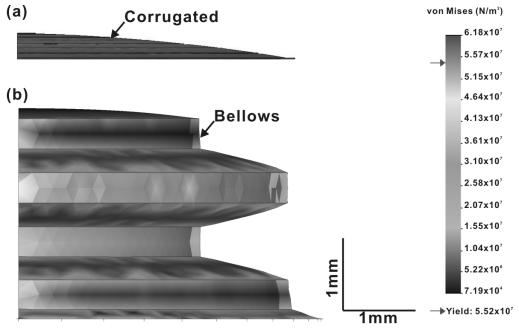

Figure 4: FEM analyses showing stress distributions for (a) Parylene corrugated membrane and (b) bellows.

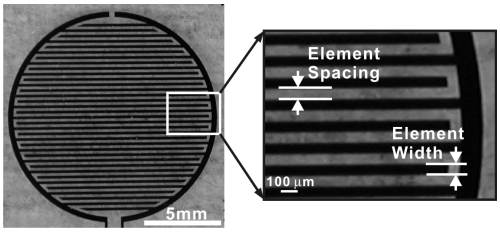

Figure 5: Interdigitated Pt/Ti electrode layout for electro-chemical actuator.

Molded Parylene Bellows

The bellows fabrication process, dissolvable PEG mold, and fabricated bellows are shown in Figures 6 and 7. First, a PDMS master mold was formed by stacking four 400 µm thick PDMS sheets each containing a ring that provides one half of a corrugation. Then liquid PEG was applied to the PDMS mold and degassed (Figure 6a). After cooling, the molded PEG was released from the PDMS mold and coated with 10 µm of Parylene C (Figure 6b). Finally, the PEG was dissolved in heated DI water (85°C) to release the Parylene bellows (Figure 6c).

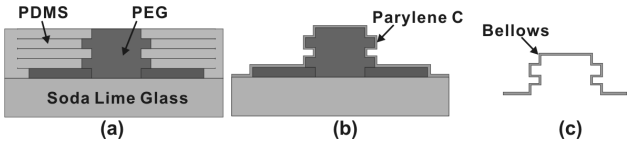

Figure 6: Molding process flow for Parylene bellows.

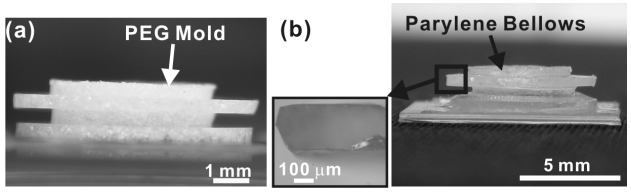

Figure 7: Molded Parylene bellows: (a) PEG mold and (b) released Parylene bellows with close up of the top convolution.

Actuator Assembly

The electrode base and Parylene bellows were assembled to complete the electrochemical actuator as shown in Figure 8. The bellows half of the actuator was first filled with DI water and attached to the pump base using double-coated pressure sensitive adhesive film.

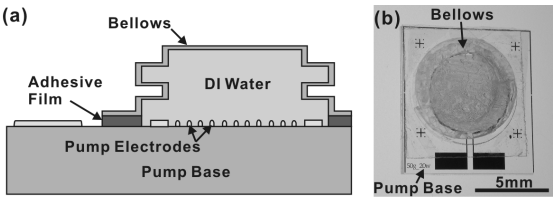

Figure 8: Pump actuator: (a) schematic diagram of the 2-part assembly and (b) image of assembled actuator.

RESULTS AND DISCUSSION

Mechanical Characterization of the Bellows

Load-deflection experiments were performed and compared well with FEM results but not the linear bellows approximation (Figure 9). The large mismatch in the latter is likely due to the nonlinear nature of Parylene, scaling effects, and low number of bellows convolutions (n = 1.5). Experimentally, an average maximum deflection of 1.78 mm was obtained under 3.45 kPa (0.5 psi) applied pressure. This relatively large deformation under low pressure loading compared to the starting height of the bellows (1.6 mm) implies low pumping resistance of the Parylene bellows.

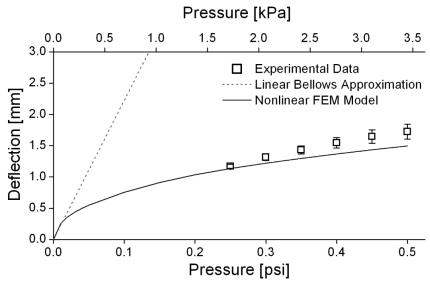

Figure 9: Comparison of experimental data with theory and nonlinear FEM model (mean±SE, n=4).

Pump Efficiency

Multiple interdigitated electrolysis electrode designs (varying element spacing and width) were investigated to determine design parameters for optimal pumping efficiency in an effort to decrease power consumption for wireless operation in chronic *in vivo* studies (Table1). The gas generation rate and pumping efficiency (under 1 mA) were measured and calculated, respectively (Figure 10). These experiments were performed on only the electrodes which were clamped in a custom testing fixture. Gas generation and thus pumping efficiency improved with increasing element spacing; a peak efficiency was identified in relation to current density and element width. Elements measuring 50µm wide and having 100µm spacing yielded the best performance (efficiency of ~80% compared to 49% [3]).

Table 1: Electrode parameters for electrolysis pump optimization.

Element With (µm)	Element Spacing (µm)	Electrode Area (mm^2)
20	20	20.0
20	50	11.2
20	100	7.0
50	20	29.8
50	50	20.2
50	100	14.2
100	20	34.6
100	50	27.4
100	100	21.4

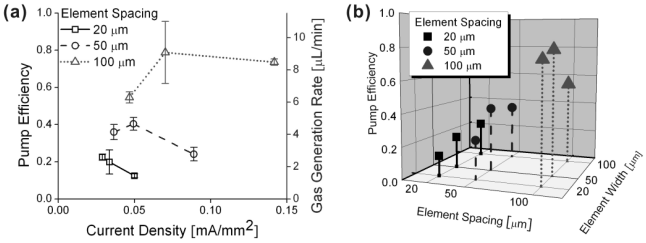

Figure 10: Pump geometry optimization based on the current-controlled flow delivery showing the relation of (a) pump efficiency vs. current density (mean±SE, n=4) and (b) pump efficiency vs. element spacing and width.

Flow Rate, Gas Recombination, and Real-time Pressure Measurement

The performance of the assembled actuator was evaluated using a laser-machined test fixture (Figure 11). Flow rates up to 6.5 µL/min (1 mA) were obtained and the corresponding pump efficiency was calculated (Figure 12). No flow was measured below 0.2 mA due to the presence of Pt which catalyzes gas recombination into water. In Figure 13, a typical accumulated volume curve is shown that illustrates the effect of recombination after the applied current is turned off. The measured recombination rate was 8.0 µL/min.

Normal intraocular pressure (IOP) in humans measures 5-22 mmHg (15.5±2.6 mmHg (mean±SD)) [7] whereas glaucoma patients suffer from elevated IOP levels (>22 mmHg). Thus, real-time measurements of electrolysis chamber pressure were collected at different currents and ON-OFF operation of the pump was evaluated (Figure 14). The fluctuation of the pressure in the pump reservoir can be repeatedly controlled by current and is suitable for pumping against normal and abnormal IOPs.

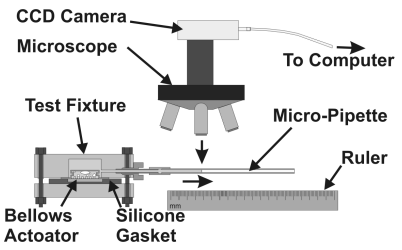

Figure 11: Flow rate testing apparatus diagram.

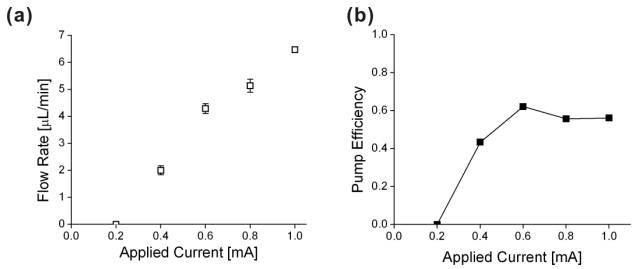

Figure 12: Pump testing: (a) current-controlled delivery collected from 20 μm width and 100 μm gap device (mean±SE, n=4) and (b) calculated pump efficiency.

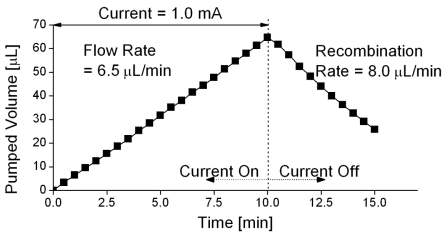

Figure 13: Typical gas recombination behavior for the actuator.

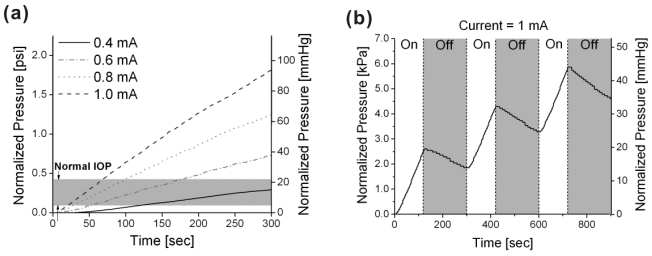

Figure 14: Real-time pressure measurement (a) in actuator chamber and (b) during ON (2min)-OFF (3 min) operation.

Wireless Operation

Wireless operation by inductive power transfer was successfully demonstrated using a custom apparatus developed for biomedical implants (2MHz) [8]. Flow rates up to 2 μL/min (I_{rms} = 0.24 mA) with hand-wound Litz wire coils and 3.4 μL/min (I_{rms} = 0.78 mA) with coils printed on PCBs were achieved.

CONCLUSION

We developed an electrochemical actuator with a Parylene bellows suitable for intraocular drug delivery and other implantable micro drug pump applications. The design, modeling, fabrication, and benchtop testing were described. An optimized electrode dimension with improved pump efficiency approaching 80% was obtained. Parylene bellows fabricated by the PEG molding technique provided low pumping resistance and large deflection (> 1.5 mm). Current-controlled flow rate and chamber pressure were also measured. Wireless operation was demonstrated (up to 3.4 μL/min) and will enable, for the first time, practical chronic *in vivo* operation and therapeutic delivery of ophthalmic drugs in animal models of ocular disease. Complete drug delivery system integration is currently underway.

ACKNOWLEDGEMENTS

This work was funded in part by the NIH/NEI under award number R21EY018490. The authors would like to thank Drs. D. Zhu, T. Hoang, T. Givrad, D. Holschneider, J.-M. Maarek, and members of the Biomedical Microsystems Lab at University of Southern California.

REFERENCES

[1] C. R. Neagu, J. G. E. Gardeniers, M. Elwenspoek, and J. J. Kelly, "An electrochemical microactuator: Principle and first results," *J. Microelectromech. S.*, vol. 5, pp. 2-9, 1996.

[2] J. Xie, Y. N. Miao, J. Shih, Q. He, J. Liu, Y. C. Tai, and T. D. Lee, "An electrochemical pumping system for on-chip gradient generation," *Anal. Chem.*, vol. 76, pp. 3756-3763, 2004.

[3] P.-Y. Li, J. Shih, R. Lo, S. Saati, R. Agrawal, M. S. Humayun, Y. C. Tai, and E. Meng, "An electrochemical intraocular drug delivery device," *Sens. Actuators A-Phys.*, vol. 143, pp. 41-48, 2008.

[4] A. J. Bard and L. R. Faulkner, *Electrochemical Methods-Fundamentals and Applications*, 2nd ed. Hoboken: John Wiley & Sons, Inc., 2001.

[5] C. Belmont and H. H. Girault, "Coplanar interdigitated band electrodes for electrosynthesis," *Journal of Applied Electrochemistry*, vol. 24, pp. 719-724, 1994.

[6] J. A. Haringx, "Instability of Bellows Subjected to Internal Pressure," *Phillips Research Reports*, vol. 7, pp. 189-196, 1952.

[7] C. R. Ethier, M. Johnson, and J. Ruberti, "Ocular biomechanics and biotransport," *Annu. Rev. Biomed. Eng.*, vol. 6, pp. 249-273, 2004.

[8] W. H. Moore, D. P. Holschneider, T. K. Givrad, and J. M. I. Maarek, "Transcutaneous RF-Powered Implantable Minipump Driven by a Class-E Transmitter," *Biomedical Engineering, IEEE Transactions on*, vol. 53, pp. 1705-1708, 2006.

CONTACT

* P.-Y. Li, tel: +1-213-821-3949; poyingli@usc.edu